

Three-Dimensional Finite Element Modeling of Magnetic Flux Leakage Technique for Detection of Defects in Carbon Steel Plates

W. Sharatchandra Singh, S. Thirunavukkarasu, S. Mahadevan, *B.P.C. Rao, C. K. Mukhopadhyay and T. Jayakumar

Non Destructive Evaluation Division, Indira Gandhi Centre for Atomic Research, Kalpakkam-603102, Tamil Nadu

*Corresponding author:

Dr. B.P.C. Rao

Head, EMSI Section, NDE Division

Indira Gandhi Centre for Atomic Research

Kalpakkam – 603 102, Tamil Nadu, INDIA

Phone: +91 44 27480232 Fax: +91 44 27480356

e-mail: bpcrao@igcar.gov.in

Abstract: Three-dimensional finite element (FE) modeling of magnetic flux leakage (MFL) technique has been performed using COMSOL 3.4 for prediction of leakage fields from surface and sub-surface defects in 12 mm thick carbon steel plate. The tangential and normal components of leakage fields have been predicted to study the influence of defect location and depth on the detectability of sub-surface defects by the MFL technique. The effect of lift-off on MFL signals has also been studied for enhancing the reliability of detection of defects.

Keywords: Finite element modeling, magnetic flux leakage, sub-surface defects, carbon steel plate.

1. Introduction

Magnetic flux leakage (MFL) technique is widely used for non-destructive detection and evaluation of surface and sub-surface defects in ferromagnetic objects such as long oil and gas pipelines, storage tank floors and wire ropes [1]. In this technique, the test object is magnetized to near saturation flux density. The presence of a defect in the test object acts as localized magnetic dipole with effective magnetic moment opposite to the applied magnetic field. This results in a proportion of the magnetic field leak out of the object surface. This leakage flux is detected by magnetic sensors and used to estimate the shape and size of the defect [2].

One advantage of MFL technique is its ability to model the leakage field from defect. The modeling enables the study of field/defect interactions and helps in better understanding and effective utilization of the MFL technique. MFL modeling is based on two methods:

- Analytical method
- Finite element (FE) method

In analytical method, defects are assumed as magnetic dipoles developed at the walls of the defect. The MFL signals are calculated from the magnetic field of the magnetic dipoles. The analytical modeling offers closed form solution but it is limited to simple geometries.

In FE method, the leakage field is obtained by solving the relevant Maxwell's equations with appropriate boundary conditions. The FE method is capable of modeling of nonlinear problems and irregular geometries which are difficult to be modeled analytically.

MFL modeling using FE method was first carried out by Lord and Huang [3]. This was followed by a series of significant works by Lord *et al* [4] and Atherton *et al* [5]. In these early works, only 2D FE with comparatively coarse mesh elements was employed. L. Chen *et al* [6] used 3D FE to simulate the effect of complex corrosion on MFL signals from a 12 mm thick steel plate and found that the relative positions of the complex corrosion pits affects the magnitude of MFL signals. H. Zuoying *et al* [7] used 3D FE

to analyze the relation between defect parameters (length, width and depth) and MFL signals of surface defects. The effects of different pit corner geometries on MFL signals were studied by V. Babbar *et al* [8] who found that the MFL signals are influenced by the sharpness of the pit corner. M. Katoh *et al* [9] analyzed the influence of air gap between the magnetizing yoke and specimen and also specimen thickness on the detectability of flaw. In the above studies, the effects of defect location and depth on the detectability of sub-surface defects in the MFL technique have not been discussed. Moreover, sub-surface defects are difficult to simulate experimentally.

This paper presents the three-dimensional FE modeling of leakage magnetic fields from surface and sub-surface defects of different dimensions in 12 mm thick carbon steel plate. The details of 3D model and results of FE study of the effects of depth location and depth on the detectability of sub-surface defects in the MFL technique are discussed in the paper. The influence of lift-off value to the MFL signals is also studied.

2. Three-Dimensional Finite Element Modeling

COMSOL 3.4 Multiphysics software package [10] in magnetostatic mode has been used for 3D FE modeling. Figure 1 shows the mesh generated for the geometry which consists of a permanent magnet (length 90 mm, cross-sectional area 55 x 50 mm² and leg spacing 70 mm) and carbon steel plate (length 240 mm, breadth 150 mm and thickness 12 mm) with 15 mm long slot. The permanent magnet is used for magnetic induction to magnetize the plate to near saturation.

Treating the MFL problem as magnetostatic, the following equations have been used with usual notations:

$$\nabla \cdot \mathbf{B} = 0 \quad (1)$$

$$\nabla \times \mathbf{H} = \mathbf{J} \quad (2)$$

$$\mathbf{B} = \nabla \times \mathbf{A} \quad (3)$$

$$\mathbf{B} = \mu_0 \mu_r \mathbf{H} = \mu_0 \mathbf{H} + \mu_0 \mathbf{M} \quad (4)$$

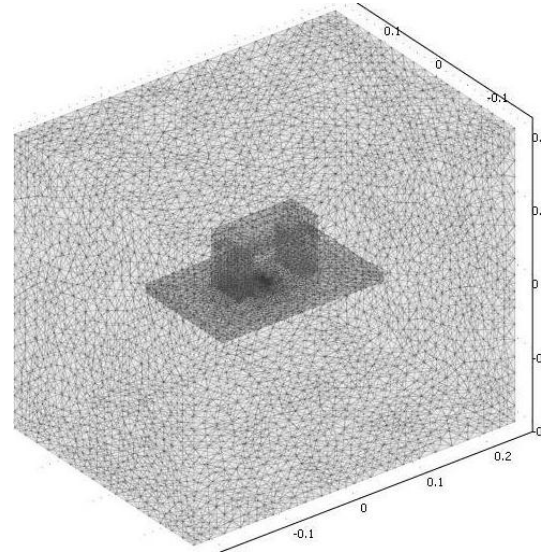


Figure 1. Mesh structure of 3D MFL finite element modeling.

Assuming the magnetic permeability of carbon steel as isotropic, equation (2) can be written as

$$\nabla \times \left(\frac{1}{\mu_0 \mu_r} \nabla \times \mathbf{A} \right) = \mathbf{J} \quad (5)$$

Equation (5) is solved in three dimensions using the FE method. A magnetization level of 100000 A/m is assumed. The relative magnetic permeability of magnet and carbon steel are assumed as 1000 and 100, respectively. The electric insulation ($\mathbf{n} \times \mathbf{H} = 0$) boundary condition has been applied at the boundaries. The boundary conditions are set in a region sufficiently far from the region of interest so as to not significantly affect the results. The mesh consists of 214984 tetrahedral elements. The mesh element size near the slot is chosen to be small (0.02) to obtain a more accurate result. The computation time for solving the above equation (5) with 1383232 degrees of freedom is approximately 2 hours in dual core 64 bit processor workstation with 8 GB primary memory. The magnetic vector potential is computed for surface and sub-surface slots and the tangential (B_x) and normal (B_z) components of the leakage flux at different lift-offs have been predicted. A normalized arrow plot of magnetic flux density of a 4 mm deep sub-surface slot

located at 2 mm below the surface is shown in figure 2. As can be seen, the magnetic field is diverted at the defect region and leaked out of the defect surface.

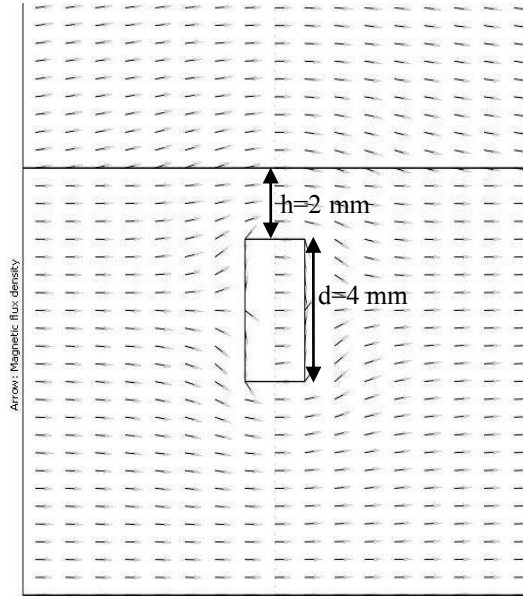
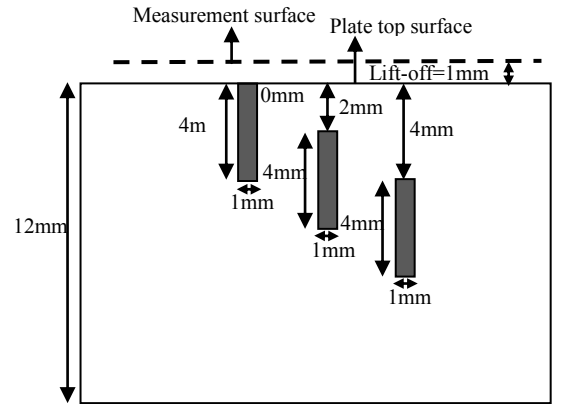


Figure 2. FE model predicted arrow plot for a 4 mm deep sub-surface slot located at 2 mm below the plate surface.

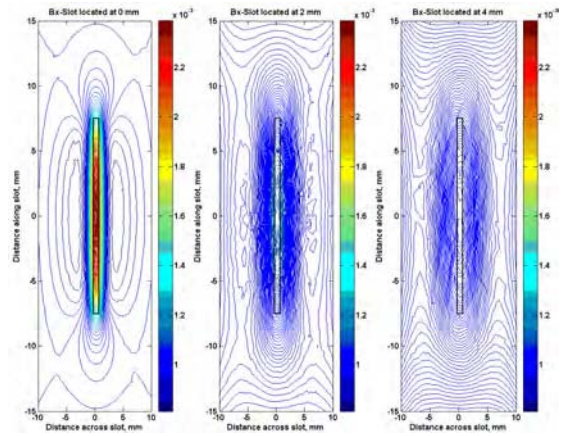
3. Modeling Results and Discussion

3.1 Effect of defect location

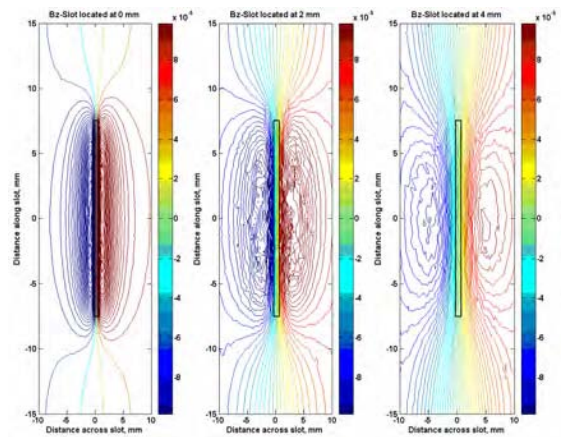
Figure 3a shows the carbon steel plate with slots (length 15 mm, width 1 mm, depth 4 mm) located at 0 mm, 2 mm and 4 mm below the plate surface. Figures 3b and 3c show the model predicted contour plots of B_x and B_z components of leakage fields for the slots. The intensities of both the components of leakage fields for the slot are found to decrease with the increase in location below the surface while the lateral spread of signals are found to increase.



a)



b)



c)

Figure 3a) Slots of 4 mm depth located at 0 mm, 2 mm and 4 mm below the plate surface and its FE model predicted contour plots of b) B_x and c) B_z components of leakage fields.

3.2 Effect of defect depth

Figure 4a shows the carbon steel plate with sub-surface slots (length 15 mm, width 1 mm) of different depths such as 2 mm, 4 mm and 6 mm located at 2 mm below the plate surface. Figure 4b shows the model predicted contour plots of B_x component of the leakage fields for the slots. As can be seen, the intensity of leakage fields for the same slot location increases with the increase in slot depth. The lateral spread of signals is also found to increase.

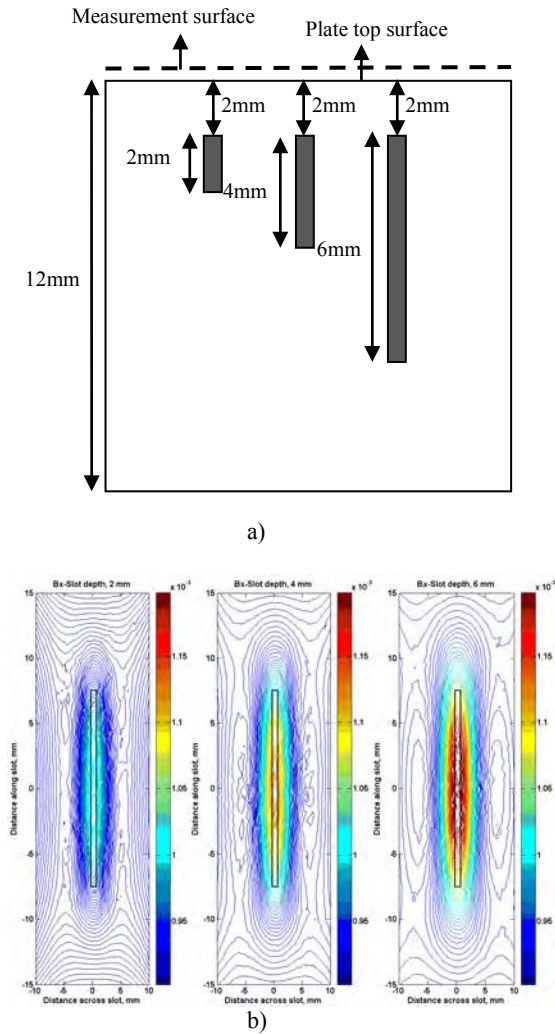


Figure 4a) Sub-surface slots of 2 mm, 4 mm and 6 mm depth located at 2 mm below the plate surface in 12 thick steel plate and b) its FE model predicted contour plots of B_x component of leakage fields.

3.3 Effect of lift-off

The B_x component of MFL signals of a sub-surface slot (length 15 mm, width 1 mm and depth 4 mm) located at 2 mm below the plate surface is predicted across the center of the slot for different lift-offs as shown in figure 5. As expected, the intensity of MFL signals decreases with the increase in lift-off.

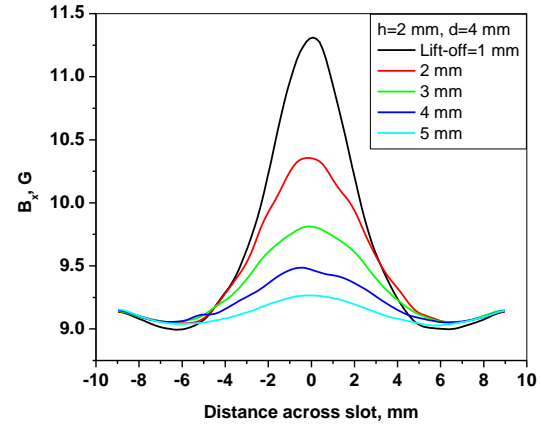


Figure 5. B_x component of MFL signals for a 4 mm deep sub-surface slot located at 2 mm below the plate surface for different lift-offs.

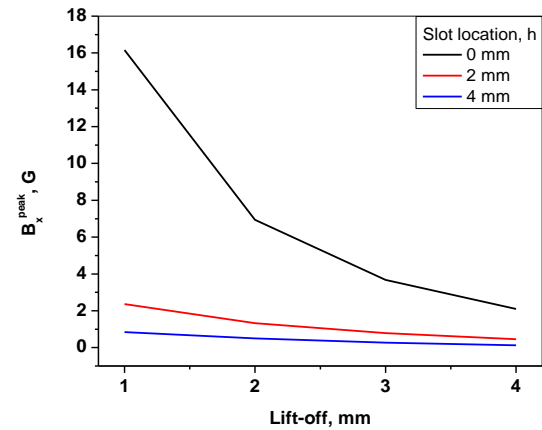


Figure 6. FE model predicted peak amplitudes (B_x^{peak}) for a 4 mm deep slot located at 0 mm, 2 mm and 4 mm below the plate surface as a function of lift-off.

The peak amplitudes (B_x^{peak}) of B_x component of MFL signals are calculated for a slot (length 15 mm, width 1 mm and depth 4 mm) of three locations at 0 mm, 2 mm and 4 mm below the plate surface. Figure 6 shows the

variation of B_x^{peak} amplitudes as a function of lift-off. The MFL signal amplitude is found to decrease with the increase in lift-off for the same slot location. It is also observed that the decrease of signal amplitude is found to be more prominent for the surface slot ($h=0$ mm) as compared to that of sub-surface slots ($h=2$ mm, 4 mm).

Thus, the 3D FE modeling of leakage field enables the calculation of field/defect interactions which are helpful for better understanding and effective utilization of the MFL technique for detection and evaluation of defects in carbon steel plates.

4. Conclusions

Three-dimensional FE modeling has been performed to study the effects of defect location and depth on the detectability of sub-surface defects in the MFL technique. The intensity of leakage fields is found to decrease with the increase in defect location below the surface while the intensity of leakage fields increases with the increase in defect depth. The effect of lift-off on MFL signals is also analyzed for enhancing the reliable detection of defects. Features such as peak amplitudes, full width at half maximum (FWHM), slope at half maximum, B_x - B_z loop area, etc. extracted from the model predicted signals may be useful for characterisation of defects. Efforts are underway.

5. References

1. S.S. Udpa and P.O. Moore, *Nondestructive Testing Handbook*, **volume 5** – Electromagnetic Testing, ASNT 3rd Edition, p. 230, 2004.
2. W. Sharatchandra Singh, B. P. C. Rao, S. Vaidyanathan, T. Jayakumar and Baldev Raj, “Detection of Leakage Magnetic Flux from Near-side and Far-side Defects in Carbon Steel Plates using Giant-magnetoresistive Sensor”, *Measurement Science and Technology*, **volume 19**, 015702 (8 pp), 2008.
3. W. Lord and J. H. Hwang, “Finite element modeling of magnetic field-defect interactions”, *ASTM J. Testing & Evaluation*, **volume 3**, pp. 21-25, 1975.
4. W. Lord, J.M. Bridges, W. Yen and R. Palanisamy, “Residual and active leakage fields

around defects in ferromagnetic materials”, *Material Evaluation*, **volume 36**, p. 47-54, 1978.

5. D.L. Atherton and M.G. Daly, “Finite element calculations of magnetic flux leakage detector signals”, *NDT International*, **volume 20**, pp. 235-238, 1987.

6. L. Chen, P. Que, Z. Huang and T. Jin, “Three-dimensional finite element analysis of magnetic flux leakage signals caused by Transmission Pipeline complex corrosion”, *Journal of the Japan Petroleum Institute*, **volume 48**, 5, 2005, pp. 314-318.

7. H. Zuoying, Q. Peiwen and C. Liang, “3D FEM analysis in magnetic flux leakage method”, *NDT & E International*, **volume 39**, pp. 61-66, 2006.

8. V. Babbar and L. Clapham, “Modeling the effects of pit corner geometry on magnetic flux leakage signals”, *Research in Nondestructive Evaluation*, **volume 17**, pp. 161-175, 2006.

9. M. Katoh, K. Nishio and T. Yamaguchi, “FEM study on the influence of air gap and specimen thickness on the detectability of flaw in the yoke method”, *NDT & E International*, **volume 33**, pp. 333-339, 2000.

10. COMSOL: Multiphysics modeling and simulation, www.comsol.com.

6. Acknowledgements

Authors thank Dr. Baldev Raj, Director, Indira Gandhi Centre for Atomic Research, Kalpakkam for encouragement.